GEOLOGY

E: geology@geosociety.org
W: geosociety.org/gsa
T: @geosociety

Early formation and taphonomic significance of kaolinite associated with Burgess Shale fossils

Tracking no: G48067R

Authors:
Ross Anderson (University of Oxford), Nicholas Tosca (University of Oxford), Erin Saupe, Jon Wade (University of Oxford), and Derek Briggs (Yale University)

Abstract:
The role of minerals in Burgess Shale-type fossilization is controversial, particularly that of the clay mineral kaolinite. Kaolinite may have formed on carcasses or attached to them as they decayed, stabilizing organic matter. Alternatively, kaolinite may have formed during metamorphism, playing no role in the preservation of soft tissues. Evaluating the formation and taphonomic role of kaolinite is difficult, because the mineralogy of Burgess Shale-type fossils is incompletely known. We used in situ selected-area X-Ray diffraction to constrain the mineralogy of fossils from the classic Burgess Shale Formation. Fossils are distinguished from the matrix that surrounds them by the presence of dolomite, kaolinite, and pyrite. Chlorite may be more abundant in the matrix. The preferential survival of kaolinite in association with fossils evidences early diagenetic clay-organic interactions that protected the clay from metamorphic transformation. Kaolinite likely played a crucial role in fossilization, inhibiting the growth of heterotrophic bacteria and aiding polymerization of soft tissue biomolecules. This may result in biases in soft-tissue preservation to areas and times where kaolinite was prevalent.

Early formation and taphonomic significance of kaolinite associated with Burgess Shale fossils

Ross P. Anderson[1,2], Nicholas J. Tosca[3], Erin E. Saupe[2], Jon Wade[2], Derek E.G. Briggs[4]

[1] *All Souls College, University of Oxford, Oxford, OX1 4AL, UK*

[2] *Department of Earth Sciences, University of Oxford, Oxford, OX1 3AN, UK*

[3] *Department of Earth Sciences, University of Cambridge, Cambridge, CB2 3EQ, UK*

[4] *Department of Earth and Planetary Sciences, Yale University, New Haven, Connecticut 06511, USA*

ABSTRACT

The role of minerals in Burgess Shale-type fossilization is controversial, particularly that of the clay mineral kaolinite. Kaolinite may have formed on carcasses or attached to them as they decayed, stabilizing organic matter. Alternatively, kaolinite may have formed during metamorphism, playing no role in the preservation of soft tissues. Evaluating the formation and taphonomic role of kaolinite is difficult, because the mineralogy of Burgess Shale-type fossils is incompletely known. We used *in situ* selected-area X-Ray diffraction to constrain the mineralogy of fossils from the classic Burgess Shale Formation. Fossils are distinguished from the matrix that surrounds them by the presence of dolomite, kaolinite, and pyrite. Chlorite may be more abundant in the matrix. The preferential survival of kaolinite in association with fossils evidences early diagenetic clay-organic interactions that protected the clay from metamorphic transformation. Kaolinite likely played a crucial role in fossilization, inhibiting the growth of heterotrophic bacteria and aiding polymerization of soft tissue biomolecules. This may result in biases in soft-tissue preservation to areas and times where kaolinite was prevalent.

INTRODUCTION

Burgess Shale-type (BST) fossil assemblages provide an exceptional wealth of biological information about Cambrian ecosystems, preserving soft tissues and entire soft-bodied organisms. Consequently, much effort has been expended on investigating their taphonomy (Gaines, 2014). BST fossils are preserved primarily as carbonaceous compressions (Butterfield, 1990; 1995). However, diagenetic mineralization may have stabilized organic matter or replicated morphology. In the Burgess Shale Formation, for example, a role for apatite and pyrite (known to replicate soft tissues: Briggs 2003) has been documented (Gaines, 2014 and references therein), and clay minerals, specifically the aluminosilicate kaolinite, have been posited to preserve morphological details by precipitating on/attaching to the surface of decaying carcasses (Orr et al., 1998). Resolving the role of minerals in BST fossilization is key to understanding any environmental bias in these fossil assemblages and interpreting the Cambrian fossil record.

The role of clay minerals is particularly controversial due to uncertainties over the timing of their formation. Variation in the abundance of clays on anatomical features of fossils from the Burgess Shale Formation may reflect original tissue chemistry: different clays formed in association with/attached to different decaying tissues, facilitating their preservation (Orr et al., 1998). Alternatively, clays may be a product of greenschist metamorphism that occurred millions of years post fossilization (Powell, 2003) and played no role in the initial conservation of soft tissues. In this case variation may be a product of precipitation from an evolving metamorphic fluid in the space created by the progressive volatilization of individual tissues (Butterfield et al., 2007; Page et al., 2008). However, metamorphism likely resulted in convergence of the fossilized tissues to a kerogen-like composition (e.g., Briggs and Summons, 2014), reducing compositional differences to a level insufficient for differential volatilization. If clays played a role in fossilization in the Burgess Shale and other BST localities, then the BST fossil record may be biased to particular environments/times when clay formation was favored.

The primary difficulty in determining when clays formed and evaluating their role in fossilization is our limited knowledge of the precise mineralogy of BST fossils. There is little constraint on mineralogical differences between anatomical features, or between fossils and their matrices. We document for the first time the distribution of minerals across specimens from the Burgess Shale Formation by applying *in situ* selective-area X-Ray diffraction (XRD) and statistically evaluate mineralogical differences between fossils and matrices. These data complement elemental maps and resolve the formational history of clays. They also constrain the distribution of other taphonomically important minerals, e.g., pyrite. Understanding the role that clays and other minerals played in Burgess Shale fossilization affords critical insight into the taphonomy of this and other BST assemblages, which are crucial to our understanding of early animals.

MATERIALS AND METHODS

Elemental and mineralogical data were obtained from Burgess Shale Formation specimens of the stem-polychaete *Canadia* (n=3), the stem-arthropods *Marrella* (n=3) and *Opabinia* (n=2), the stem-priapulid *Ottoia* (n=4), and the stem-chordate *Pikaia* (n=3). Elemental maps were generated via scanning electron microscopy-energy dispersive X-Ray spectroscopy (SEM-EDS), and mineralogical data were obtained using non-destructive *in situ* selected-area XRD. The XRD irradiated area was controlled using various configurations of incident beam optics (minimum area is 7×1 mm; for locations of selected-area XRD analyses, see DR). Relative mineral abundances were calculated using the reference intensity ratio method (Snyder and Bish, 1989) with *Highscore* software (referred to as “Highscore data”). This method provides imprecise identification and quantification of specific clays, so we confirmed the identification of kaolinite—the principal clay argued by Orr et al. (1998) to have played a role in fossilization—by analysis of its ~7 Å peak (Moore and Reynolds, 1997) with *Fityk* software (referred to as “Fityk data”). Statistical analyses were executed in the R programming language to explore the relationship between selected-area type (i.e., fossil or matrix) and mineralogical composition. For details, see GSA Data Repository (DR), Section 1.

RESULTS

Selected-area XRD (Figs. 1, 2, DR) revealed that chlorite, muscovite, and quartz are the most abundant minerals in both fossils and their matrices, together with minor amounts of calcite, dolomite, kaolinite, and pyrite.

To assess whether specific minerals are preferentially associated with fossils versus their matrices, we performed mixed effect logistic regression models using a partially Bayesian method (Chung et al., 2013). The relative abundance of each mineral using Highscore data was included as a predictor of selected-area type (i.e., fossil or matrix) in every combination, resulting in 128 possible models including one with no fixed effects (DR Tables S2 and S3). Twenty of the 128 models received non-trivial weight (Akaike’s Information Criterion, ΔAIC < 10). Dolomite, kaolinite, and pyrite are significantly more abundant in fossils in all non-trivial models whereas chlorite is more abundant in matrices than fossils. The relative abundances of calcite, muscovite, and quartz were indistinguishable between fossils and their matrices; confidence interval estimates for these minerals were inclusive of zero for most non-trivial models. To compensate for the fact that the predictors are compositional, we ran a suite of models without quartz as a predictor, producing 8 models of non-trivial weight of a possible 64 (DR Tables S4 and S5). Results were equivalent to the models inclusive of quartz: dolomite, kaolinite, and pyrite were significantly more abundant in fossils, whereas chlorite was more abundant in matrices in all non-trivial models. Calcite and muscovite were indistinguishable between fossils and their matrices.

We also used partially Bayesian mixed effect logistic models to determine whether the presence/absence of minerals alone could distinguish between fossils and their matrices. We considered only the presence/absence of calcite, dolomite, kaolinite, and pyrite, because chlorite, muscovite, and quartz are present in nearly all (>98%) selected-area analyses. Of 16 possible models fit using presence/absence derived from Highscore data, six received non-trivial support (DR Tables S6 and S7). The only predictors with confidence intervals exclusive of zero in these models were kaolinite and pyrite, both of which are positively and significantly associated with fossils. The highest-ranking model included only kaolinite and pyrite. Moreover, kaolinite was also found to be positively and significantly associated with fossils when identified using the Fityk data (DR Table S7).

SEM-EDS elemental distributions (DR Figs. S1–S15) also distinguish fossils from their matrices and are consistent with the mineralogies identified by selected-area XRD. Aluminum is a major constituent of both kaolinite and muscovite. Features of the digestive system are enriched in aluminum relative to the rest of the fossil. Iron indicative of pyrite often co-varies with carbon, e.g., in the eyes of *Opabinia*.

DISCUSSION

The data provide statistical support that fossils are distinguished from their matrices by the presence and higher abundances of dolomite, kaolinite and pyrite, and the lower abundance of chlorite. Pyrite is expected to be associated with fossils (Briggs, 2003: DR Section 3.4 for discussion of other minerals). However, the association of kaolinite with fossils provides data that illuminate its formation (Fig. 3). If kaolinite formed as a retrograde phase, following a metamorphic mineral that precipitated into voids left by the volatilization of soft-tissues (Butterfield et al., 2007; Page et al., 2008), it would likely occur in similar abundance in both fossils and matrices, as this mode of formation involves replacement of illite/muscovite (present in similar abundances in fossils and matrices) in the presence of adequate fluid flow (Nieto et al., 2005). The association of kaolinite with fossils and not matrices, in contrast, supports an early diagenetic origin during carcass decay.

Although kaolinite that formed early in diagenesis is unlikely to have survived the metamorphic history of the Burgess Shale Formation (the isochemical nature of most metamorphic reactions in pelitic rocks, and the high aluminum and potassium content of the strata, favor a near quantitative conversion of kaolinite to illite/muscovite and chlorite: Powell, 2003), chemical interactions between kaolinite and organic matter provide a viable mechanism for its selective survival on fossils. Bonding of kaolinite to organic matter during early diagenesis could have been facilitated in various ways, and interactions are likely to be localized and dependent on specific functional groups (Theng, 1974). Local decreases in pH with initial decay (Briggs and Kear, 1993) could have resulted in a net positive charge on the surface of the organic matter, promoting bonding with the negatively charged edge sites of kaolinite (e.g., Skujinš et al., 1974; Theng, 1974; Yu et al., 2013). Kaolinite edge sites (10–20% of its surface area: Theng, 1974) behave as Lewis acids; they are likely to have remained negatively charged even at relatively low pH (Sposito, 1984; Brady et al., 1996). Alternatively, cation incorporation/exchange into the organic matter could have increased its isoelectric point (thereby establishing a positive surface charge depending on pore water pH: Stotzky, 1980), or may have provided a bridge to overcome electrostatic repulsion (Phoenix et al., 2003). Strong binding of kaolinite to the decaying carcass protected its edge sites from dissolution by aqueous fluids during metamorphism, allowing a small fraction of the mineral to survive. The data do not, however, resolve whether the mineral precipitated directly on carcasses or bonded to them as pre-existing kaolinite. Experimental and theoretical work has shown both silicate formation on organic substrates (Wallace and Schiffbauer, 2016) and the propensity of pre-existing kaolinite to attach to organic substrates including decaying tissues in experiments (Martin et al., 2004; Playter et al., 2017).

Given that kaolinite interacted with decaying carcasses, its chemical properties likely played a key role in soft-tissue fossilization (e.g., Butterfield, 1990; 1995). Experimental evidence indicates that kaolinite inhibits the growth of bacterial degraders (likely due to the toxicity of its constiuent Al^{3+}: DR Section 2), in particular heterotrophic bacteria involved in the decay of marine animals (McMahon et al., 2016). Kaolinite may also stabilize decaying carcasses through its bonds with their organic matter. The bonding properties of kaolinite edge sites (e.g., bond strength and *p*Ka) are unique among clays (Sposito, 1984; Brady et al., 1996) and have been invoked to explain the polymerization (Solomon and Rosser, 1965) and adsorption (Skujinš et al., 1974; Theng, 1974) of organic molecules, as well as the tendency of kaolinite to trigger kerogen maturation upon pyrolysis (Pan et al., 2010). Surface sites located along basal planes could also stabilize pre-existing organic cross-links via the donation of electrons, reducing double bonds and further promoting fossilization (Stimler and Tanzer, 1977). Experiments have shown decay-resistance through tissue polymerization via kaolinite-organic interactions (Wilson and Butterfield, 2014; Naimark et al., 2018).

Clay concentrations may have impeded decay more widely by distinct but complementary processes. Globally, sediments hosting BST assemblages are enriched in the iron-rich clay berthierine, a product of kaolinite exposed to pore-water Fe^{2+} early in diagenesis (Anderson et al., 2018; Saleh et al., 2019). Consistent with this observation, chlorite (iron-rich: chamosite), the metamorphic product of berthierine, is more abundant in matrices than fossils in almost all our XRD analyses. Bonding to organic matter, which limited transformations of kaolinite including berthierine formation, accounts for this pattern (fig. 3, DR Section 3.2). Like kaolinite, berthierine (probably due to its toxic constituent Fe^{2+}) impedes growth of bacteria involved in decay (McMahon et al., 2016; DR Section 2). Thus, preservation may be enhanced by the presence of berthierine transformed from kaolinite in the environs of the carcass, as well as kaolinite attached to it. Soft-tissue preservation in the Burgess Shale and other Cambrian BST assemblages is, therefore, likely to be biased to environs where kaolinite is readily available. Kaolinite forms in regions of high drainage and low pH today—commonly in the tropics (Wilson, 2013). Consistent with this observation, BST assemblages almost always occur in tropical paleolatitudes (Hendricks et al., 2008).

No bias toward the fossilization of particular phylogenetic groups was detected in this work: small sample size precluded assessment of statistical differences in mineralogy between taxa, but kaolinite was present on all specimens including, a stem annelid, a variety of ecdysozoans, and a stem-chordate. Further, evidence suggests kaolinite-organic interactions have played a role in the fossilization of other eukaryotes and even cyanobacteria (Anderson et al., 2020). However, our data do not rule out a bias toward the fossilization of specific animal tissues: more labile tissues, which decay rapidly and drive pH lower faster, may be more likely to bond with kaolinite (Skujinš et al., 1974; Theng, 1974; Briggs and Kear, 1993; Yu et al., 2013). SEM-EDS data detected enhanced aluminum enrichments associated with labile digestive organs, indicating that initial kaolinite may have been preferentially associated with these tissues, but sample sizes prevented assessment of these enrichments with XRD data.

Despite the evidence of mineral-organic interactions during decay, they were not the only factors controlling Cambrian BST fossilization. Sediment composition (including clay content: Anderson et al., 2018; Saleh et al, 2019), oxidant availability, and the formation of authigenic cements were also important (Gaines, 2014), and their relative contribution presumably varied by setting. The evidence suggests that the mineralogical distinctions between fossils and their associated matrices in the Burgess Shale Formation, specifically the association of kaolinite with fossils, reflect formation in early diagenesis, resolving the controversy over the timing of kaolinite formation and its role in fossilization.

ACKNOWLEDGEMENTS

D. Erwin, M. Florence, S. Butts, and J. Utrup facilitated access to fossils. We are grateful to S. Kearns for conducting SEM-EDS at the University of Bristol. K. Clayton assisted with XRD analyses. We thank K. Konhauser and J. Schiffbauer for helpful reviews, as well as N. Butterfield, S. Kearns, and two anonymous reviewers for comments on an earlier version. The Leverhulme Trust (PLP-2015-286), a Mid-America Paleontological Society Student Award, NASA (NNA13AA90A and NNX14AP10H), and the Yale Institute for Biospheric Studies and Peabody Museum supported this work.

REFERENCES

Anderson, R.P., Tosca, N.J., Cinque, G., Frogley, M.D., Lekkas, I., Akey, A., Hughes, G.M., Bergmann, K.D., Knoll, A.H., and Briggs, D.E.G., 2020, Aluminosilicate haloes preserve complex life approximately 800 million years ago: Interface Focus, v. 10, 20200011.

Anderson, R.P., Tosca, N.J., Gaines, R.R., Mongiardino Koch, N., and Briggs, D.E.G., 2018, A mineralogical signature of Burgess Shale-type fossilization: Geology, v. 46, p. 347–350, https://doi.org/10.1130/G39941.1.

Brady, P.V, Cygan, R.T., and Nagy, K.L., 1996, Molecular controls on kaolinite surface charge: Journal of Colloid and Interface Science, v. 183, p. 356–364 **183**, 356–364, https://doi.org/10.1006/jcis.1996.0557.

Briggs, D.E.G., 2003, The role of decay and mineralization in the preservation of soft-bodied fossils: Annual Review of Earth and Planetary Sciences, v. 31, p. 275–301, https://doi.org/10.1146/annurev.earth.31.100901.144746.

Briggs, D.E.G., and Kear, A.J., 1993, Decay and preservation of polychaetes: Taphonomic thresholds in soft-bodied organisms: Paleobiology, v. 19, p. 107–135, https://doi.org/10.1017/S0094837300012343.

Briggs, D.E.G., and Summons, R.E., 2014, Ancient biomolecules: Their origins, fossilization, and role in revealing the history of life: BioEssays, v. 36, p. 482–490, https://doi.org/10.1002/bies.201400010.

Butterfield, N.J., 1990, Organic preservation of non-mineralizing organisms and the taphonomy of the Burgess Shale: Paleobiology, v. 16, p. 272–286, https:/doi.org/10.1017/S0094837300009994.

Butterfield, N.J., 1995, Secular distribution of Burgess-Shale-type preservation: Lethaia, v. 28, no. 1, p. 1–13, https://doi.org/10.1111/j.1502-3931.1995.tb01587.x.

Butterfield, N.J., Balthasar, U., and Wilson, L.A., 2007, Fossil diagenesis in the Burgess Shale: Palaeontology, v. 50, p. 537–543, https://doi.org/10.1111/j.1475-4983.2007.00656.x.

Chung Y., Rabe-Hesketh, S., Dorie, V., Gelman, A., Liu, J., 2013, A nondegenerate penalized liklihood estimator for variance parameters in multilevel models: Psychometrika, v. 78, p. 685–709, https://doi.org/10.1007/s11336-013-9329-2.

Gaines, R.R., 2014, Burgess Shale-type preservation and its distribution in space and time: Paleontological Society Papers, v. 20, p. 123–146.

Hendricks, J.R., Lieberman, B.S., and Stigall, A.L., 2008, Using GIS to study palaeobiogeographic and macroevolutionary patterns in soft-bodied Cambrian arthropods: Palaeogeography, Palaeoclimatology, Palaeoecology, v. 264, p. 163–175, https:// doi .org /10 .1016 /j .palaeo .2008 .04.014.

Martin, D., Briggs, D.E.G., and Parkes, R.J., 2004, Experimental attachment of sediment particles to invertebrate eggs and the preservation of soft-bodied fossils: Journal of the Geological Society of London, v. 161, p. 735–738, https://doi.org/10.1144/0016-764903-164.

McMahon, S., Anderson, R.P., Saupe, E.E., and Briggs, D.E.G., 2016, Experimental evidence that clay inhibits bacterial decomposers: Implications for preservation of organic fossils: Geology, v. 44, p. 867–870, https://doi.org/10.1130/G38454.1.

Moore, D.M., and Reynolds, R.C., 1997, X-Ray Diffraction and the Identification and Analysis of Clay Minerals: Oxford University Press, Oxford, 378pp.

Naimark, E.B., Kalinina, M., Shokurov, A., Markov, A., Zaytseva, L., and Boeva, N., 2018, Mineral composition of host sediments influences the fossilization of soft tissues: Canadian Journal of Earth Sciences, v. 55, p. 1271–1283, https://doi.org/10.1139/cjes-2017-0237.

Nieto, F., Pilar Mata, M., Bauluz, B., Giorgetti, G., Árkai, P., and Peacor, D.R., 2005, Retrograde diagenesis, a widespread process on a regional scale: Clay Minerals, v. 40, p. 93–104, https://doi.org/10.1180/0009855054010158.

Orr, P.J., Briggs, D.E.G., and Kearns, S.L., 1998, Cambrian Burgess Shale animals replicated in clay minerals: Science, v. 281, p. 1173–1175, https://doi.org/10.1126/science.281.5380.1173.

Page, A., Gabbott, S.E., Wilby, P.R., and Zalasiewicz, J.A., 2008, Ubiquitous Burgess Shale-style "clay templates" in low-grade metamorphic mudrocks: Geology, v. 36, p. 855–858, https://doi.org/10.1130/G24991A.1.

Pan, C., Geng, A., Zhong, N, and Liu, J., 2010, Kerogen pyrolysis in the presence and absence of water and minerals: Steranes and triterpenoids: Fuel, v. 89, p. 336–345, https://doi.org/10.1016/j.fuel.2009.06.032.

Phoenix, V.R., Konhauser, K.O., and Ferris, F.G., 2003, Experimental study of iron and silica immobilization by bacteria in mixed Fe-Si systems: Implications for microbial silicification in hotsprings: Canadian Journal of Earth Sciences, v. 40, p. 1669–1678, https://doi.org/10.1139/E03-044.

Playter, T.L., Konhauser, K.O., Hodgson, C.A., Owttrim, G., Mloszewska, A., Sutherland, B., Bekker, A., Zonneveld, J.-P., Pemberton, S.G., and Gingras, M.K., 2017, Microbe-clay interactions as a mechanism for the preservation of organic matter and trace metal biosignatures in black shales: Chemical Geology, v. 459, p. 75–90, https://doi.org/10.1016/j.chemgeo.2017.04.007

Powell, W., 2003, Greenschist-facies metamorphism of the Burgess Shale and its implications for models of fossil formation and preservation: Canadian Journal of Earth Sciences, v. 40, p. 13–25, https://doi.org/10.1139/e02-103.

Saleh, F. Pittet, B., Perrillat, J.-P., Lefebvre, B., 2019, Orbital control on exceptional fossil preservation: Geology, v. 47, p. 103–106, https://doi.org/10.1130/G45598.1.

Skujinš, J., Pukite, A., and McLaren, A.D., 1974, Adsorption and activity of chitinase on kaolinite: Soil Biology and Biochemistry, v. 6, p. 179–182, https://doi.org/10.1016/0038-0717(74)90024-8.

Snyder, R.L., and Bish, D.L., 1989, Quantitative analysis, in Bish, D.L., and Pose, J.E., eds., Modern Powder Diffraction: Reviews in Mineralogy, v. 20, Mineralogical Society of America, p. 101–144.

Solomon, D.H., and Rosser, M.J., 1965, Reactions catalyzed by minerals. Part 1. Polymerization of styrene: Journal of Applied Polymer Science, v. 9, p. 1261–1271, https://doi.org/10.1002/app/1965.070090407.

Sposito, G., 1984, The surface chemistry of soils: Oxford, Oxford University Press, 234 p.

Stimler, N.P., and Tanzer, M.L., 1977, Location of the intermolecular cross linking sites in collagen *in* Friedman, M., eds. Protein crosslinking. Advances in Experimental Medicine and Biology, Volume 86: Boston, Springer, p. 675–697.

Stotzky, G., 1980, Surface interactions between clay minerals and microbes, viruses and soluble organics, and the importance of these interactions to the ecology of microbes in soil *in* Berkeley, R.C.W., Lynch, J.M, Melling, J., Rutter, P.R., Vincent, B., eds. Microbial adhesion to surfaces: Ellis Horwood, Chichester, p. 231–247.

Theng, B.K.G., 1974, The chemistry of clay-organic reactions: New York, John Wiley and Sons, 343 p.

Wallace, A.F., and Schiffbauer, J.D., 2016, Model systems as probes of organic-mineral interactions in ancient environments: Geological Society of America Abstracts with Programs, v. 48, https://doi.org/10.1130/abs/2016AM-285087.

Wilson, M.J. 2013 Rock forming minerals, 3C: Clay minerals: London, The Geological Society of London, 724 p.

Wilson, L.A., and Butterfield, N.J., 2014, Sediment effects on the preservation of Burgess Shale-type compression fossils: Palaios, v. 29, p. 145–154, https://doi.org/10.2110/palo.2013.075.

Yu, W.H., Li, N., Tong, D.S., Zhou, C.H., Lin, C.X., and Xu, C.Y., 2013, Adsorption of proteins and nucleic acids on clay minerals and their interactions: A review: Applied Clay Science, v. 80–81, p. 443–452, https://doi.org/10.1016/j.clay.2013.06.003.

FIGURE CAPTIONS

Figure 1: Representative selected-area XRD and SEM-EDS maps of *Marrella* (USNM 229990). A: Photograph with selected-areas covering the fossil (numbers refer to XRD analyses: DR Table S1). B–C: SEM-EDS maps showing the distribution of Al, C, Si, and Ca, Fe, P. D: Representative selected-area XRD (fossil analysis from selected-area 1 in A; Chl=chlorite, Kaol=kaolinite, Musc=muscovite, Qtz=quartz).

Figure 2: Box plots showing mineralogy across specimens recorded by selected-area XRD using Highscore data.

Figure 3: Fate of kaolinite through early diagenesis and metamorphism in fossils versus matrices.

Differences in the relative importance of the transformations (thickness of arrows denotes importance) produced the distinct fossil/matrix mineralogy.

[1] GSA Data Repository item 202Xxxx, Further methodological particulars, antibacterial properties of clays, other minerals with distinct fossil/matrix distributions, summaries of mineralogy by taxon, data tables, statistical summaries, and light/SEM-EDS images of fossil specimens showing XRD selected-areas is available online at www.geosociety.org/pubs/ft20XX.htm, or on request from editing@geosociety.org or Documents Secretary, GSA, P.O. Box 9140, Boulder, CO 80301, USA.

Figure 1

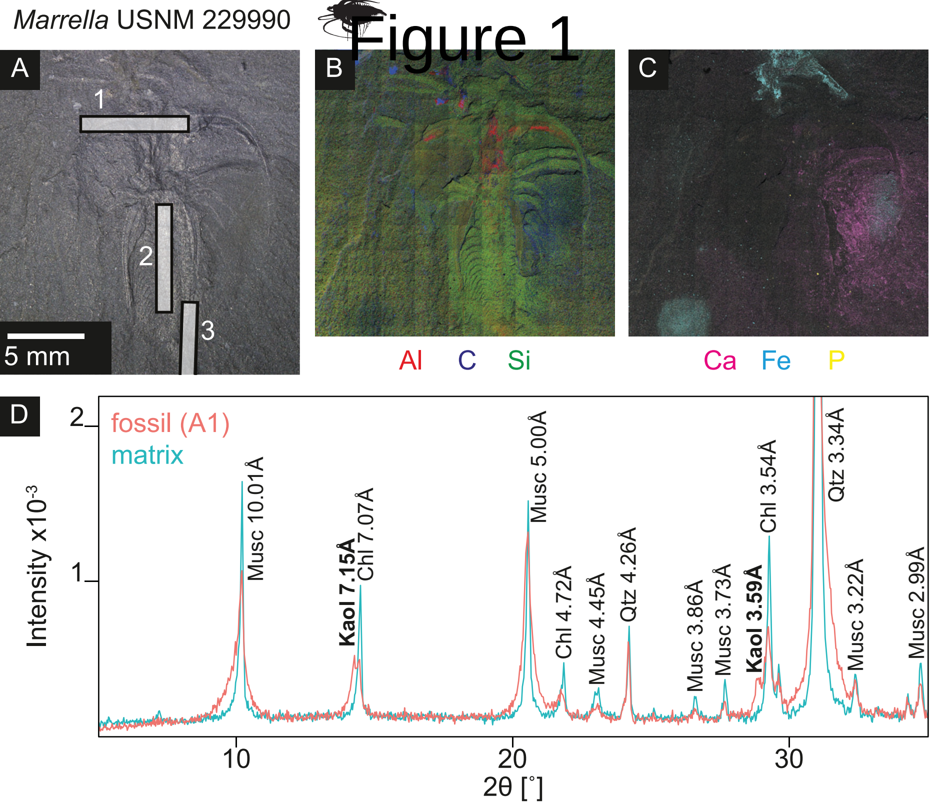
Marrella USNM 229990
A
1
2
3
5 mm
B
Al
C
Si
C
Ca
Fe
P
D
fossil (A1)
matrix
Intensity x10-3
2
1
Musc 10.01Å
Kaol 7.15Å
Chl 7.07Å
Musc 5.00Å
Chl 4.72Å
Musc 4.45Å
Qtz 4.26Å
Musc 3.86Å
Musc 3.73Å
Kaol 3.59Å
Chl 3.54Å
Qtz 3.34Å
Musc 3.22Å
Musc 2.99Å
10
20
30
2θ [˚]

Figure 2

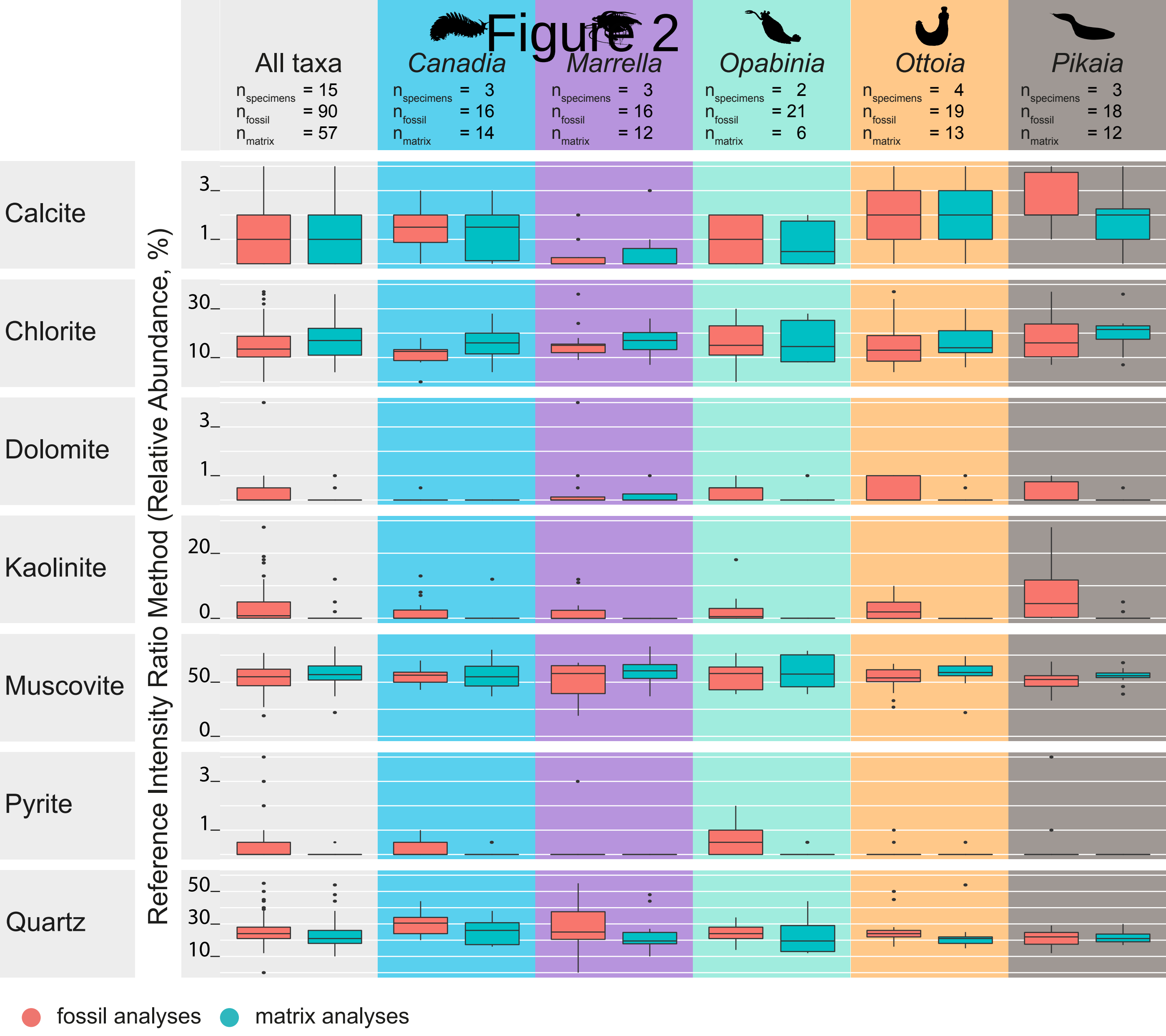
All taxa
$n_{specimens}$ = 15
n_{fossil} = 90
n_{matrix} = 57
Canadia
$n_{specimens}$ = 3
n_{fossil} = 16
n_{matrix} = 14
Marrella
$n_{specimens}$ = 3
n_{fossil} = 16
n_{matrix} = 12
Opabinia
$n_{specimens}$ = 2
n_{fossil} = 21
n_{matrix} = 6
Ottoia
$n_{specimens}$ = 4
n_{fossil} = 19
n_{matrix} = 13
Pikaia
$n_{specimens}$ = 3
n_{fossil} = 18
n_{matrix} = 12
Calcite
3
1
Chlorite
30
10
Dolomite
3
1
Kaolinite
20
0
Muscovite
50
0
Pyrite
3
1
Quartz
50
30
10
Reference Intensity Ratio Method (Relative Abundance, %)
● fossil analyses
● matrix analyses

Figure 3

Fate of kaolinite